Supporting Information

Two-dimensional $SiAs_2$: metal-free photocatalysts for overall water splitting with ultrahigh carrier mobility and pronounced light absorption

Kai Zheng,[a,#] Heping Cui,[a,#] Houcai Luo,[a] Jiabing Yu,[a] Shaogang Wang,[a] Chunjian Tan, [a] Liming Wang,[a] Xiandong Li,[a] Luqi Tao,[a] and Xianping Chen,*[a]

[a)] *Key Laboratory of Optoelectronic Technology & Systems, Education Ministry of China, Chongqing University and College of Optoelectronic Engineering, State Key Laboratory of Power Transmission Equipment & System Security and New Technology, Chongqing University, 400044 Chongqing, China.*

 # These authors contributed equally to this work.

** To whom correspondence should be addressed: xianpingchen@cqu.edu.cn*

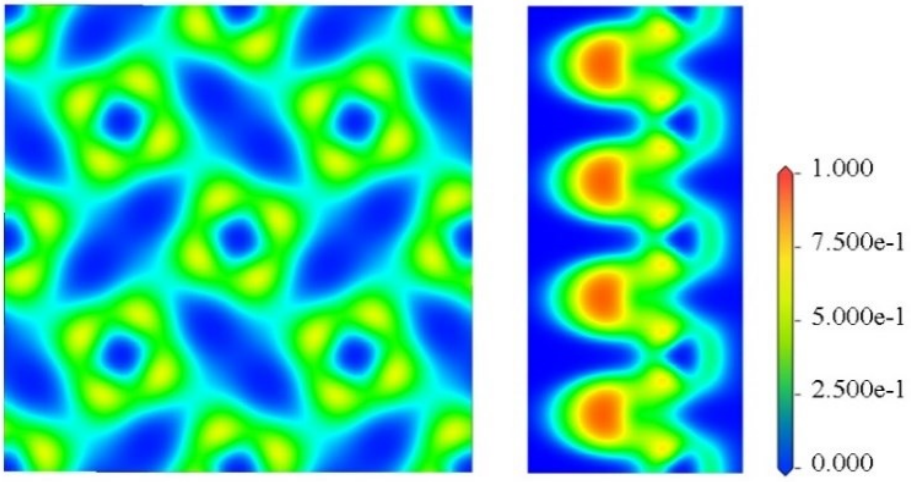

Figure S1. Electron localization functional of penta-$SiAs_2$ monolayer.

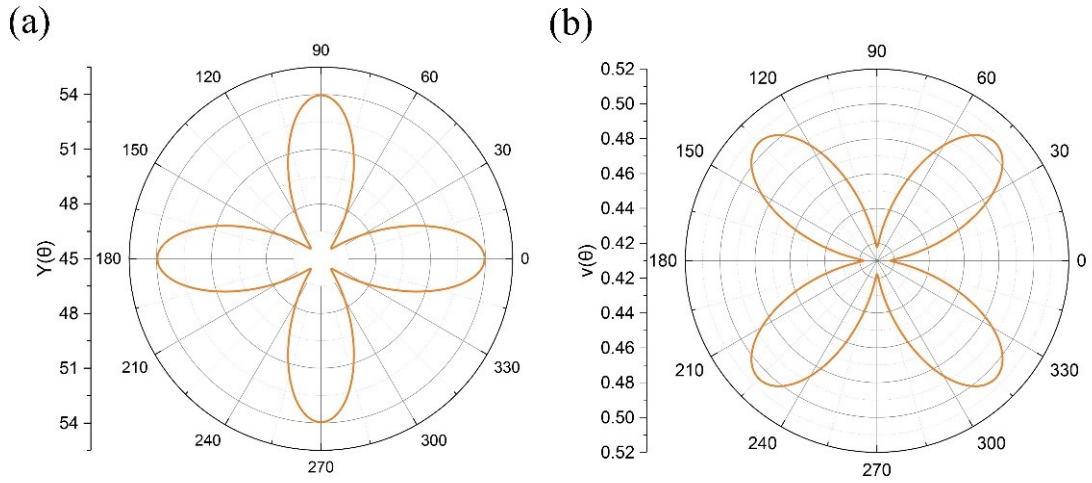

Figure S2. The orientation dependent Young's moduli and Poisson's ratio of penta-$SiAs_2$.

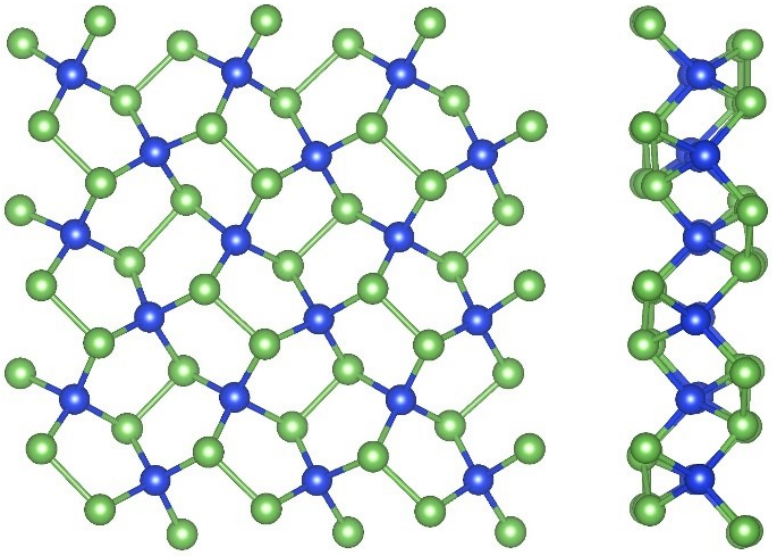

Figure S3. Snapshots of AIMD simulations of penta-$SiAs_2$ monolayer at the end of 2 ps with the temperature controlled at 300 K from top view and side view.

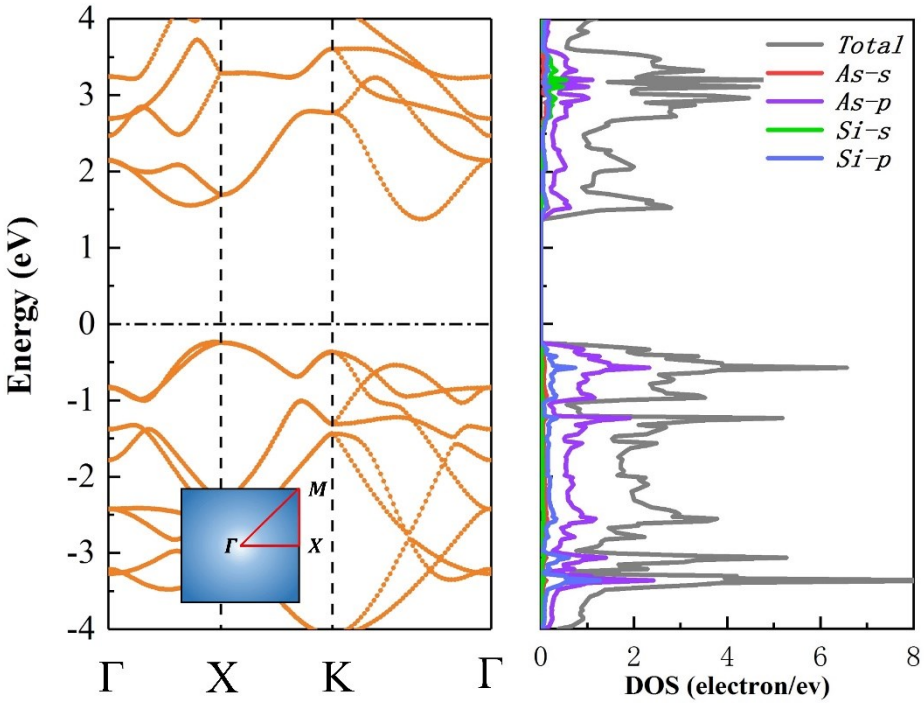

Figure S4. Band structure of monolayer panta-$SiAs_2$ with the GGA-PBE functional.

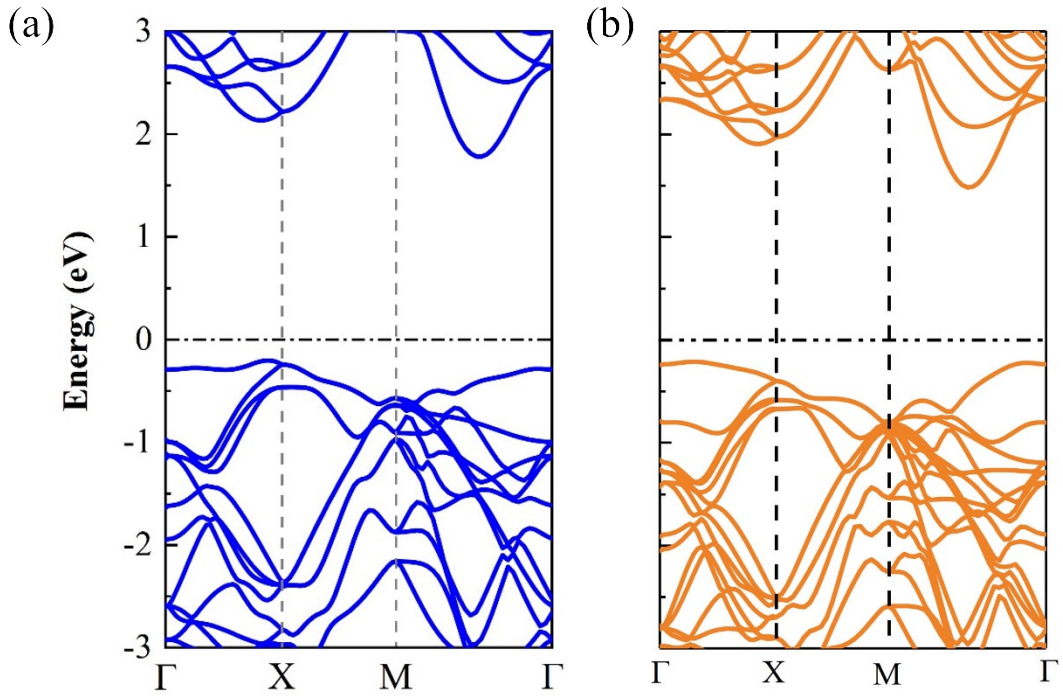

Figure S5. Band structure of (a） bilayer and (b) trilayer panta-SiAs2 with the HSE06 functional.

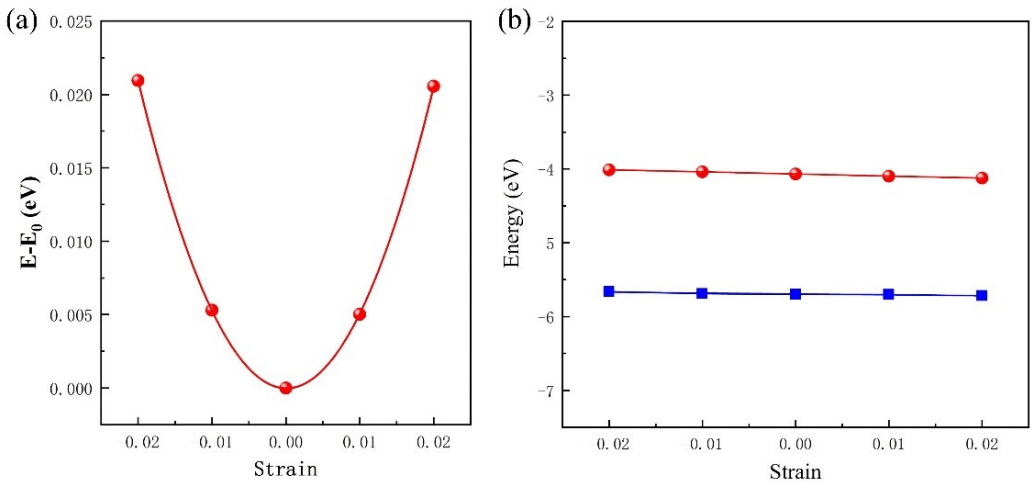

Figure S6. Strain energy curves for penta-$SiAs_2$ monolayer. Linear fittings of the CBM and VBM shift with respect to the lattice dilation or compression in transport directions.

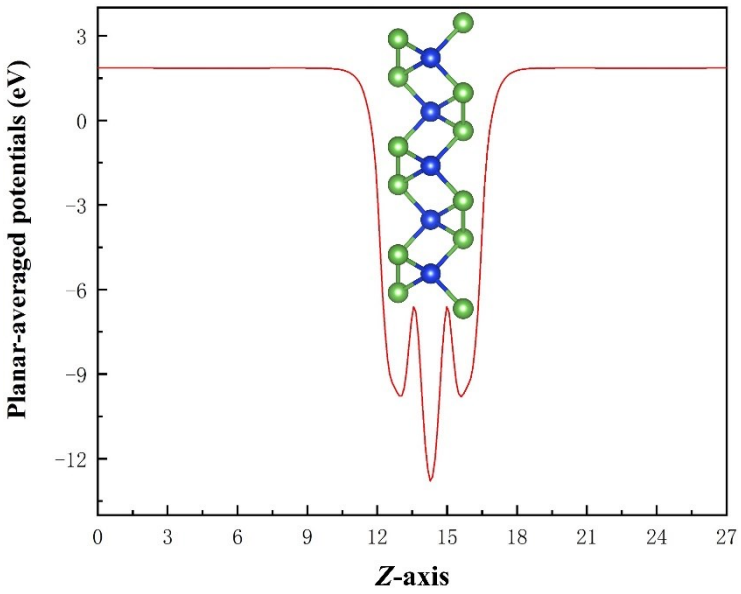

Figure S7. Planar-averaged potential along the Z-axis direction for penta-$SiAs_2$ monolayer.

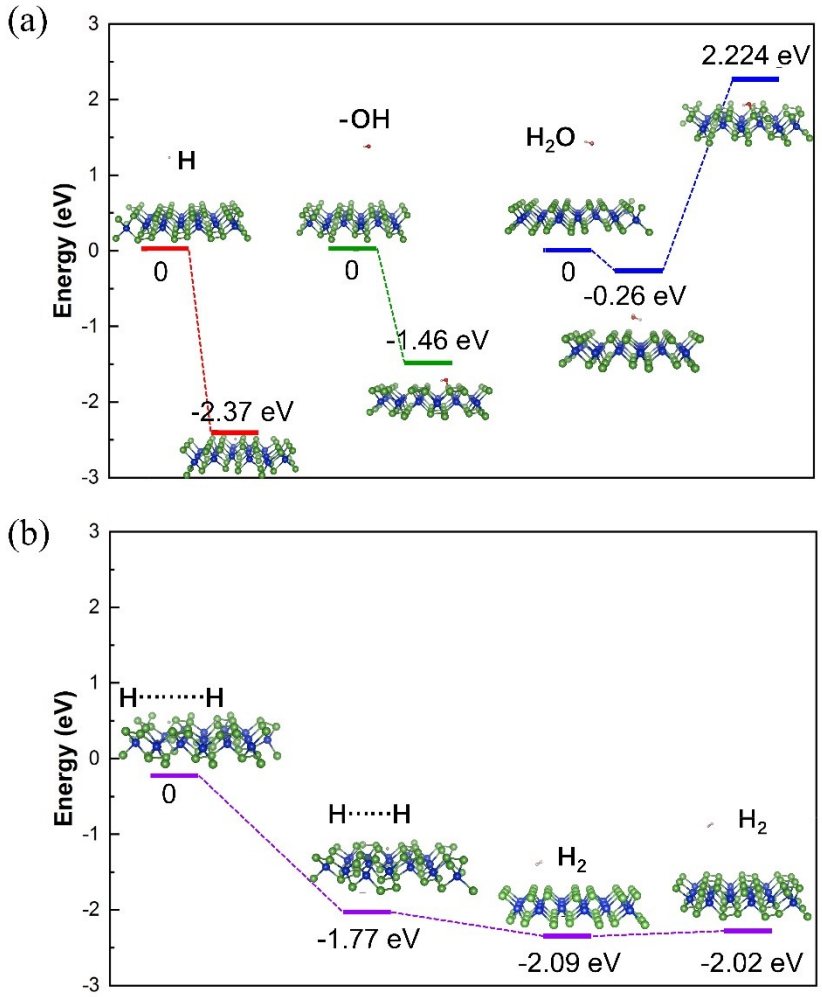

Fig. S8 (a) Energy differences between the configurations of before and after adsorption H, OH, and H_2O, and decomposition of H_2O on monolayer $SiAs_2$. (b) Energy pathways of releasing of hydrogen on 2D $SiAs_2$. The red and white spheres represent the O and H atoms, respectively.